

Structure and dynamics of vibrated granular chains: Comparison to equilibrium polymers

Kevin Safford,¹ Yacov Kantor,² Mehran Kardar,³ and Arshad Kudrolli¹

¹*Department of Physics, Clark University, Worcester, Massachusetts 01610, USA*

²*Raymond and Beverly Sackler School of Physics and Astronomy, Tel Aviv University, Tel Aviv 69978, Israel*

³*Department of Physics, Massachusetts Institute of Technology, Cambridge, Massachusetts 02139, USA*

(Received 16 January 2009; published 10 June 2009)

We show that the statistical properties of a vibrated granular bead chain are similar to standard models of polymers in equilibrium. Granular chains of length up to $N=1024$ beads were confined within a circular vibrating bed, and their configurations were imaged. To differentiate the effects of persistence and confinement on the chain, we compared with simulations of both persistent random-walk (RW) and self-avoiding walk (SAW) models. Static properties, such as the radius of gyration and structure factor, are governed for short chains ($N \leq 128$) by persistence and can be matched by those of RWs. Self-avoidance and confinement effects are both important for longer chains and the results are well described by equilibrated SAWs. We also find that the collective dynamics of the granular chain is similar to the Rouse model of polymers. In particular, as long as confinement is negligible, the center of mass of the chain diffuses with a diffusion coefficient that scales as $1/N$, and the dynamic structure factor decays exponentially in time.

DOI: [10.1103/PhysRevE.79.061304](https://doi.org/10.1103/PhysRevE.79.061304)

PACS number(s): 81.05.Rm, 05.40.-a, 82.35.Lr, 05.70.Jk

I. INTRODUCTION

A question of fundamental interest is the extent to which equilibrium statistical physics and entropic considerations apply to excited granular matter [1–4]. Because of the dissipative nature of the collisions, energy has to be constantly supplied in order to keep granular matter moving. It is plausible that under sufficiently random driving and over long enough times, a granular system will explore most of the available configurational space, such that its properties can be described by equilibrium statistics. Indeed, Edwards [2] proposed a generalized statistical mechanical approach where thermodynamic quantities are calculated from averages over grain configurations, but this approach has not been rigorously established.

An appealing system to explore this connection is a granular chain excited by a vibrated rough substrate, where the corresponding equilibrium model for polymers is well developed [5–7]. A vibrated bed is used widely in industry to transport and sort granular matter and is a convenient method to obtain a driven out-of-equilibrium steady state [8–10]. Equilibriumlike properties have been observed with spherical particles with such vibrated systems [11]. Granular chains consisting of beads connected with flexible links were introduced by Ben-Naim and co-workers [12–14] to study unknotting, radius of gyration, diffusion of rings, and entropic tightening of chains. The collapse of a polymer has been modeled using a vibrated bead chain in a thin layer of liquid which induces an attractive potential [15]. Pretins and Sisan [16] performed experiments with a chain of plastic spheres agitated by self-propelled balls to examine the applicability of a self-avoiding walk (SAW) model of polymers [5–7]. Although they observed that the end-to-end length of the plastic-sphere polymer scales with the number of links N_l as N_l^ν with an exponent of $\nu=0.75$, the maximum number of links studied was only 15. Further, the possible effect of chain persistence on the scaling properties was not explored nor was dynamics. Novel filling patterns have been shown to

occur when persistence length of an elastic wire is large compared with the container size [17–19] and may be also considered as a model system to understand crumpling [20]. Therefore, a detailed study, which examines the interplay of chain length, persistence length, and container size, is necessary.

In this paper, we investigate the structure and dynamics of a granular chain on a vibrated plate by direct imaging to test if the statistical models developed in the context of molecular polymers can be applied to such an out-of-equilibrium system. The length of the chain is varied over 3 orders of magnitude, scaling across its persistence length and the system size. For short chains, we find that a random walk (RW) with a persistence length, constrained to the same size container, is sufficient to capture the radius of gyration and the structure factor observed in the experiments. As the length of the chain is increased, avoided crossings become important, and the data are observed to be in good agreement with the simulations for a confined SAW with the same persistence length. We also examine the dynamics of the granular chain and find simple diffusive motion described by the so-called Rouse model [5]. Specifically, at short times, in a regime where the granular temperature is constant, the center of mass (CM) of the chain undergoes diffusion with a diffusion coefficient that scales inversely with the length of the chain. Further, we probe how the dynamic structure factor—which is used to characterize the chain over various length scales—evolves. The expected exponential decay is observed as long as the boundary effects are small (for short chains and short times) but is modified nontrivially by the interplay of self-avoidance and confinement.

II. METHODS

The granular chain used in the experiments consists of nickel-plated aluminum spherical beads with diameter $d=3.12$ mm connected to each other by a loose link. The bead number N ranges from 1 to 1024 in our experiments. The

links between the beads can take lengths between 0 and 1.5 mm, and the chain can have a maximum angle between two consecutive links of approximately $\pm\pi/4$ rad. The persistence length of the chain ξ_p can be related to the decay of link-angle correlations by

$$\langle \cos(\theta_n - \theta_1) \rangle = \langle \cos(\theta_2 - \theta_1) \rangle^{n-1} \equiv \exp\left[-\frac{(n-1)d}{\xi_p}\right], \quad (1)$$

where θ_n is the direction angle of the n th link between beads and angular brackets denote an average over all configurations. The first equality follows from the independence of changes in angle [21]. Thus, $\xi_p/d = -1/\ln[\langle \cos(\theta_2 - \theta_1) \rangle]$, and assuming that $\theta_n - \theta_{n-1}$ are uniformly distributed between $-\pi/4$ and $\pi/4$, we find $\langle \cos(\theta_2 - \theta_1) \rangle = 2\sqrt{2}/\pi$ and $\xi_p \approx 9.5d$.

The chain is kept inside a flat circular container with diameter $L=28.3$ cm and is therefore about $90d$ across. A layer of 1 mm steel beads is glued to the bottom of the container to create a rough surface. The roughness helps transfer energy into the chains both in the vertical and horizontal directions and prevents the formation of tightly wound spiral features discussed in Ref. [22]. Therefore, while there are aspects of granular particle dynamics that differ significantly from equilibrium [22], we focus here on properties that appear in line with statistical mechanics. An electromagnetic shaker is used to continuously vibrate the container vertically using a sinusoidal input waveform with a frequency $f=30$ Hz and peak acceleration $\Gamma=3g_E$, where g_E is the earth's gravitational acceleration. The container is monitored using an accelerometer. The acceleration is chosen so that the chain is excited sufficiently strongly to move and rearrange in a reasonable time but not so strongly that one segment of the chain can leap over another segment. That is, when seen from above, the chain can be considered a two-dimensional system at all times. Limited experiments were also performed with $\Gamma=2g_E$, $3.5g_E$, and different vibration frequencies. Similar chain structure and dynamics were observed and therefore, for simplicity, we have kept the driving parameters constant in the results reported here.

We record the motion of the chain inside the container from above with a digital camera with a pixel resolution of 1024×1024 . An example of an observed configuration is shown in Fig. 1 (insert). A frame rate of 20 Hz is used to record a movie and statistical averaging is performed over a set of ten movies each containing 2000 frames. In special cases, where particle velocity is to be determined, a higher frame rate of 1000 Hz is used to record the movies. We then use a centroid algorithm [23] to find the bead positions to within a tenth of a particle diameter. With sufficient care, we find that the error rate in identification is less than 1 in 10 000 beads.

On the numerical side, we perform Monte Carlo (MC) simulations of a two-dimensional chain of N particles. We consider an athermal system, in that the spatial configurations were either permitted, and have vanishing energy or completely forbidden. The excluded volume interaction is implemented by not allowing the distance between centers of any pair of particles to be smaller than d (hard spheres),

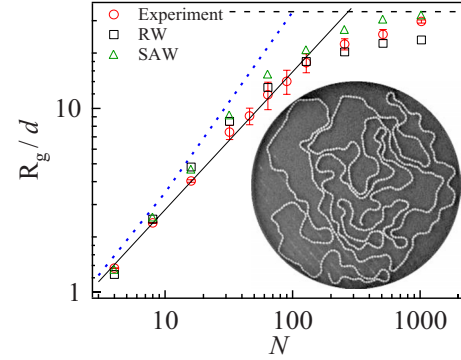


FIG. 1. (Color online) The mean radius of gyration, R_g , of the chains versus the number of beads, N . As the chains increase in size, R_g asymptotically approaches the radius of gyration of a chain uniformly distributed inside the container (indicated by the horizontal dashed line). To guide the eyes, $(N-1)^\nu$ is plotted for $\nu=3/4$ (solid line) along with $\nu=1$ (dotted line). Insert: an example of a chain configuration observed in the experiments ($N=1024$).

while the connectivity of the chain is enforced by not allowing a pair of connected particles to be separated by more than $1.4d$. Only configurations in which the angle between adjacent bonds did not exceed $\pi/4$ are permitted. We assume that the chain is confined by a circular enclosure, corresponding to the size of the experimental container.

To differentiate between the roles of persistence and self-avoidance, we also studied random (non-self-avoiding) walks. In such simulations the hard-sphere interaction between nonadjacent particles are neglected. In an elementary MC move we randomly pick a particle and attempt to move it by a small amount in a randomly chosen direction. If the new position forms a permitted configuration, the move is accepted. Otherwise, the particle remains in its original position. The size of the step is chosen to keep the move acceptance rate close to 50%; N elementary moves constitute a single MC time unit. The total length of the simulation was set to $10^3 N^2$ MC time units. In the absence of confinement, the typical relaxation times of a polymer performing diffusive dynamics are of order $N^{1+2\nu}=N^{2.5}$, where $\nu=3/4$ for SAW. Thus for small and moderate values of N our sample is very well equilibrated. For larger values of N the confinement effects strongly slow down equilibration. Nevertheless, our results for $N=512$ are well equilibrated, while we estimate that for $N=1024$ the total simulation time only slightly exceeds the equilibration time. Various quantities, such as the radius of gyration and the structure factor are then calculated for configurations obtained in the simulations and averaged.

III. STATICS

A simple measure which captures the size of an object is the radius of gyration R_g defined by

$$R_g^2 = \frac{1}{2N^2} \sum_{n=1}^N \sum_{m=1}^N \langle (\mathbf{R}_n - \mathbf{R}_m)^2 \rangle. \quad (2)$$

Here, \mathbf{R}_n is the location of the n th bead and N is the number of beads in the chain. Figure 1 shows R_g obtained

from the experiments along with the confined RW and SAW simulations with imposed persistence length. As a guide for the eyes, we have included plots of $R_g \propto (N-1)^\nu$, with $\nu=1$ and $3/4$. The former describes a straight rod with N beads, while the latter corresponds to an unconfined SAW in two dimensions [5]. At small N , the experimental data approaches a line with $\nu=1$. This is to be expected as the chains have a persistence length $\xi_p \approx 9.5d$. As N increases above ξ_p/d , the experimental data systematically starts to fall below $\nu=1$. For larger N , when the unconfined polymer size becomes comparable to that of the container, the data gradually approaches R_g of a uniform disk. According to Fig. 1, the influence of the boundaries appears for $N > 128$.

In order to separate the effects of self-avoidance on the observed R_g , we compare the data with corresponding RW simulations which have the same persistence length as the granular chains and are performed within the same container size. Interestingly, the experiments and the RW simulations compare very well for $N \leq 128$. Thus, it appears that avoided crossings are relatively unimportant for short chains but become more important as N increases, thus causing RW to underestimate R_g observed in the experiments. Therefore, the simpler RW model may be used to describe R_g for $N \leq 128$, however, the experimental data is better described by a SAW simulations at higher N .

To investigate the structure more critically and over various length scales, we next examine the static structure factor defined by

$$g(\mathbf{q}) = \frac{1}{N^2} \sum_{n=1}^N \sum_{m=1}^N \langle \exp[i\mathbf{q} \cdot (\mathbf{R}_n - \mathbf{R}_m)] \rangle. \quad (3)$$

In Fig. 3, we plot $g(q)$ as a function of the magnitude q averaged over all directions of the wave vector \mathbf{q} and all configurations in the experiments. In principle, $g(q)$ is purely real if we average over an infinite ensemble. In practice, we note that for a sufficiently large number of observed configurations, the imaginary part of $g(q)$ is small compared to the real part, and we plot only the real part in Fig. 2.

Now, $g(q)$ for an unconfined linear polymer in the limit of small and large wave number is expected [5] to scale as

$$g(q) = 1 - (qR_g)^2/2 \text{ for } qR_g \ll 1, \quad (4a)$$

$$g(q) \propto q^{-1/\nu} \text{ for } qR_g \gg 1, \quad (4b)$$

where $\nu=3/4$ in two dimensions. In the insert to Fig. 2(c), we can clearly observe that the initial decay of $g(q)$ is consistent with Eq. (4a).

The experimental data is well described by confined RW simulations over the entire range of q plotted for $N < 256$. This implies that avoided crossings are rare enough for these short chains that the volume exclusion of is not significant. Of course, as N is increased, the system becomes more dense and avoided crossings become inevitable, increasing the size of the chain. To examine if the SAW simulations compare with the experimental data, we have plotted them along with RW simulations for $N=512$ and $N=1024$ in Figs. 2(b) and 2(c). In both cases, the experimental data are better described by the SAW simulations. It is important to note that $g(q)$ is

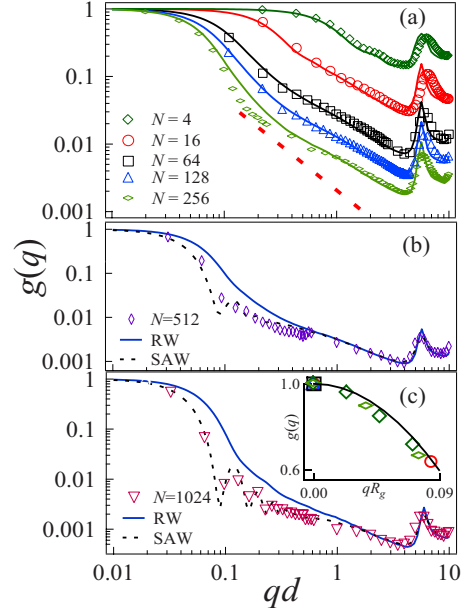


FIG. 2. (Color online) (a) The structure factor $g(q)$ of the chains obtained from the experiments (symbols) and the corresponding RW simulations (solid curves). A line with a slope $-4/3$, which corresponds to unconfined SAW with $\nu=3/4$, is also plotted to guide the eyes. The RW simulations confined to the same size container agree well with experiments for $N < 256$, but systematic deviations are observed for $N \geq 256$ because of the importance of avoided crossings. The peak near $q=2\pi/d$ corresponds to the average bead spacing of the chain. [(b) and (c)] For longer chains, the experimental $g(q)$ (circles) are better described by the SAW simulation. The insert in (c) shows that for small q the data for different N can be collapsed to a single curve according to Eq. (4a) (solid curve).

not described by Eq. (4b) for larger q because of the confinement.

IV. DYNAMICS

Next, we investigate the dynamic features of the chain by first examining the motion of its center of mass (CM). In particular, we track

$$\Delta \mathbf{R}_{\text{CM}}(t) = \mathbf{R}_{\text{CM}}(t) - \mathbf{R}_{\text{CM}}(0),$$

where $\mathbf{R}_{\text{CM}}(t)$ is the two-dimensional position of the center of mass of the chain at time t . The mean-squared displacement (MSD) of the center of mass $\langle [\Delta \mathbf{R}_{\text{CM}}(t)]^2 \rangle$ is plotted in Fig. 3. MSD is initially observed to scale linearly before saturating as chains encounter the container boundary. Fits corresponding to normal diffusion are added to guide the eyes. Clearly, shorter chains diffuse faster than longer chains. For the longest chain, the motion appears to be subdiffusive, reflecting the constraints imposed by confinement. In two dimensions, the diffusion constant D can be deduced from $\langle [\Delta \mathbf{R}_{\text{CM}}(t)]^2 \rangle = 4Dt$ and fitting the data over a range where MSD is linear. The obtained diffusion constant D_N for a chain with N beads is plotted in Fig. 4(a) as a function of N , and for moderate and large N , it is roughly proportional to N^{-1} .

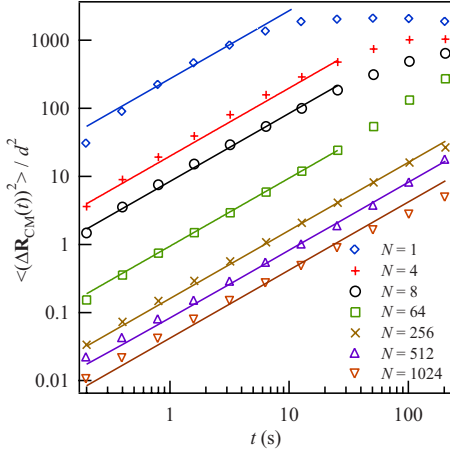


FIG. 3. (Color online) The mean-squared displacement of the CM of the granular chain, plotted against time for various chain lengths. Linear fits are plotted over a time interval before boundary effects lead to downward curvature.

According to the Rouse model for dilute polymer solutions [5]—which simply assumes that each monomer experiences a viscous drag proportional to its velocity— D_N scales with N as

$$D_N = \frac{k_B T}{N \zeta}, \quad (5)$$

where T is the temperature, k_B is the Boltzmann constant, and ζ is the friction coefficient acting on a bead. For a granular polymer, we can measure a granular temperature T_g corresponding to the in plane velocities of the beads, which may be considered to be analogous to thermal excitations of particles in a polymer system. Therefore, $k_B T \rightarrow T_g = \frac{1}{2} m \langle v^2 \rangle$, where m is the mass of a bead and v is its instantaneous velocity. T_g obtained from the experiments is shown on the right axis of Fig. 4(a) and is observed to be constant except for $N=1$. From the fit to the experimental data, we find $\zeta \approx 2.87 \times 10^{-2} \text{ N m}^{-1} \text{ s}$.

Therefore, when the granular chain moves on a vibrated rough surface and interacts through collisions with the surface, it is plausible that the plate plays the role of a thermal bath which not only supplies energy but also gives rise to an effective viscous drag. To further demonstrate the agreement with Rouse dynamics, we replot $\langle [\Delta \mathbf{R}_{\text{CM}}(t)]^2 \rangle$ for each chain against time scaled by L^2/D_N in Fig. 4(b). All the curves collapse very nearly onto a master curve further confirming that $D_N \propto N^{-1}$ over a broad range of chain lengths and time scales.

Another means of tracking the time evolution of a multi-particle system is the dynamical structure factor defined by

$$g(\mathbf{q}, t) = \frac{1}{N^2} \sum_{n,m} \langle \exp[i\mathbf{q} \cdot (\mathbf{R}_n(t) - \mathbf{R}_m(0))] \rangle.$$

For an unconfined polymer, this quantity decays in time as [5]

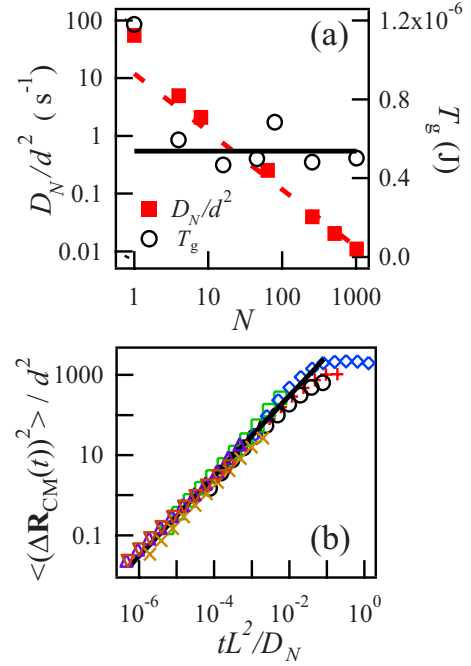


FIG. 4. (Color online) (a) The diffusion constant D_N extracted from the slopes of the lines shown in Fig. 3 and using $\langle [\Delta \mathbf{R}_{\text{CM}}(t)]^2 \rangle = 4D_N t$. $D_N \propto 1/N$ corresponds to the Rouse model and is indicated by the dashed line. The granular temperature T_g of the chain (the right axis) is observed to be approximately constant for $N > 4$. The average value of T_g for $N > 1$ is shown as a solid line. (b) The mean-squared displacements shown in Fig. 3 can be collapsed onto a single master curve when time is rescaled with the measured D_N and container size L . This shows that even long chains exhibit normal diffusion at short enough times.

$$g(q, t) \propto \exp(-D_N q^2 t). \quad (6)$$

However, such a decay is observed only if the conditions

$$qR_g \ll 1 \quad (7a)$$

and

$$|\mathbf{R}_n(t) - \mathbf{R}_m(0)| \gg R_g \quad (7b)$$

are satisfied. The above inequalities ensure that the motion of the polymer is probed at long enough times to observe its collective diffusion. These conditions are actually quite restrictive in our experiments, as the confinement by the circular boundaries severely constrain the times over which diffusion is observed, and there is only a limited range of N that leads to the decay given by Eq. (6).

In Fig. 5(a) we plot $g(q, t)/g(q, 0)$ for several N and find that the decay at large N is slower than expected from Eq. (6). Clearly at such large values the confinement of the polymer leads to rapid saturation of the displacement fluctuations. The dynamical structure factor for shorter chains of $N=8$ and $N=16$, where conditions of Eq. (7) are best met, is plotted in Fig. 5(b). Using Eq. (6) and the data of from Fig. 5(a), we can extract $D_8/d^2 = 2.1 \pm 0.1 \text{ s}^{-1}$ and $D_{16}/d^2 = 1.1 \pm 0.3 \text{ s}^{-1}$. Within experimental error bars, these values are consistent with the diffusion coefficients obtained from the motion of the center of mass in Fig. 4(a). With this choice

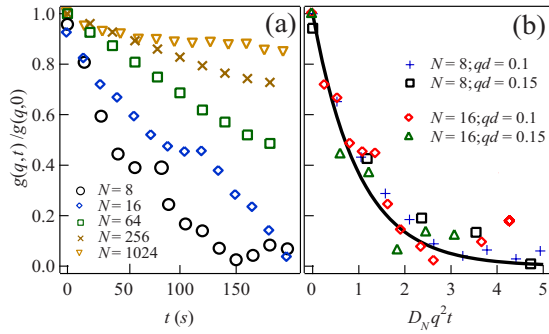


FIG. 5. (Color online) (a) The dynamical structure factor $g(q,t)/g(q,0)$ versus time for several values of N and $q=0.1d^{-1}$. For large N the decay of $g(q,t)$ is slower than exponential. (b) Here $g(q,t)/g(q,0)$ is plotted against $D_N q^2 t$ for $N=8$ and 16 for values of q that satisfy Eq. (7a). The solid line depicts $\exp(-D_N q^2 t)$.

for D_N the data is collapsed onto the single exponential curve shown in Fig. 5(b). It appears that, as long as Eq. (7) are satisfied, D_N is independent of the choice of q .

V. SUMMARY

In conclusion, we find that the configurations of vibrated granular chains are well described by standard models of

polymers when persistence length, container size, and avoided crossings are taken into account. This provides an illustrative example of a granular system where concepts of configuration entropy are useful for description of collective behavior. Furthermore, the diffusion of the center of mass scales inversely with the size of the chain and is consistent with the Rouse model of polymer dynamics. We also illustrate that the dynamic structure factor decays exponentially with time provided that the effects of confinement are negligible. Since our study implies that granular chains show properties similar to equilibrium models, it is tempting to explore experiments such as ours to understand the behavior of polymers in circumstances where direct visualization is not possible (e.g., polymer [24] and DNA molecules bound to lipid bilayers [25]).

ACKNOWLEDGMENTS

We thank Micah Veilleux for his help in performing preliminary experiments. This work was supported by the National Science Foundation under Grants No. DMR-06-05664 (K.S. and A.K.) and No. DMR-08-03315 (M.K.) and by the Israel Science Foundation under Grant No. 99/08 (Y.K.). Part of this work was carried out at the Kavli Institute for Theoretical Physics with support from NSF under Grant No. PHY05-51164 (M.K. and Y.K.).

-
- [1] H. M. Jaeger, S. P. Nagel, and R. P. Behringer, *Rev. Mod. Phys.* **68**, 1259 (1996).
 - [2] S. F. Edwards, in *Granular Matter: An Interdisciplinary Approach*, edited by A. Mehta (Springer, New York, 1994).
 - [3] P. G. de Gennes, *Rev. Mod. Phys.* **71**, S374 (1999).
 - [4] N. V. Brilliantov and T. Pöschel, *Kinetic Theory of Granular Gases* (Oxford University Press, New York, 2004).
 - [5] M. Doi and S. Edwards, *The Theory of Polymer Dynamics* (Clarendon Press, Oxford, 1986).
 - [6] P.-G. de Gennes, *Scaling Concepts in Polymer Physics* (Cornell University Press, Ithaca, 1979).
 - [7] T. A. Witten, *Rev. Mod. Phys.* **70**, 1531 (1998).
 - [8] J. S. Olafsen and J. S. Urbach, *Phys. Rev. Lett.* **81**, 4369 (1998).
 - [9] W. Losert, D. G. W. Cooper, J. Delour, A. Kudrolli, and J. P. Gollub, *Chaos* **9**, 682 (1999).
 - [10] A. Kudrolli, *Rep. Prog. Phys.* **67**, 209 (2004).
 - [11] P. M. Reis, R. A. Ingale, and M. D. Shattuck, *Phys. Rev. Lett.* **96**, 258001 (2006).
 - [12] E. Ben-Naim, Z. A. Daya, P. Vorobieff, and R. E. Ecke, *Phys. Rev. Lett.* **86**, 1414 (2001).
 - [13] Z. A. Daya, E. Ben-Naim, and R. E. Ecke, *Eur. Phys. J. E* **21**, 1 (2006).
 - [14] M. B. Hastings, Z. A. Daya, E. Ben-Naim, and R. E. Ecke, *Phys. Rev. E* **66**, 025102(R) (2002).
 - [15] B. Bammes and J. S. Olafsen, *Chaos* **14**, S9 (2004).
 - [16] J. J. Prentis and D. R. Sisan, *Phys. Rev. E* **65**, 031306 (2002).
 - [17] C. C. Donato, M. A. F. Gomes, and R. E. de Souza, *Phys. Rev. E* **66**, 015102(R) (2002).
 - [18] L. Boue, M. Adda-Bedia, A. Boudaoud, D. Cassani, Y. Couder, A. Eddi, and M. Trejo, *Phys. Rev. Lett.* **97**, 166104 (2006).
 - [19] N. Stoop, F. K. Wittel, and H. J. Herrmann, *Phys. Rev. Lett.* **101**, 094101 (2008).
 - [20] D. L. Blair and A. Kudrolli, *Phys. Rev. Lett.* **94**, 166107 (2005).
 - [21] L. D. Landau and E. M. Lifshits, *Statistical Physics: Part 1*, 3rd ed. (Butterworth-Heinemann, Oxford, 1980).
 - [22] R. E. Ecke, Z. A. Daya, M. K. Rivera, and E. Ben-Naim, *Granular Material-Based Technologies*, MRS Symposia Proceedings No. 759 (Materials Research Society, Warrendale, PA, 2003), p. 129.
 - [23] J. C. Crocker and D. G. Grier, *J. Colloid Interface Sci.* **179**, 298 (1996).
 - [24] R. Vilanove and F. Rondelez, *Phys. Rev. Lett.* **45**, 1502 (1980).
 - [25] B. Maier and J. O. Rädler, *Phys. Rev. Lett.* **82**, 1911 (1999).